

Quantification of Ovarian Granulosa Cells and Different Level Follicles in the Mouse Ovary Using Stereology Method, for Potential Application in 3D Bioengineered Ovary.

Jiahua Zheng

Second Hospital of Hebei Medical University

Jingkun Zhang

Second Hospital of Hebei Medical University

Yanpeng Tian

Second Hospital of Hebei Medical University

Yanbiao Song

Second Hospital of Hebei Medical University

Zhengwei Yang

North Sichuan Medical University

Xianghua Huang (✉ huangxh2003@163.com)

Research

Keywords: Bioengineered ovary, disector, follicles, ovarian granulosa cells, numerical density, stereology

Posted Date: May 7th, 2020

DOI: <https://doi.org/10.21203/rs.3.rs-26397/v1>

License: © ⓘ This work is licensed under a Creative Commons Attribution 4.0 International License.

[Read Full License](#)

Abstract

Background Stereology is an accurate method to obtain 3D quantitative information of microstructure based on the comprehensive observation of two-dimensional sections. Three-dimensional bioprinting of bioink to rebuild a bioengineered ovary has been proved to be a promising technique in preserving fertility. Fully understand the structure of the ovary, the distribution of the main cells and the numerical density of cells using stereology method is of great significance to the computer 3D reconstruction technology.

Results The Cavalieri method gave the estimations that the ovary was $(2.49 \pm 0.32)\text{mm}^3$, the volume fraction of cortex, medulla, follicles and ovarian granulosa cells (OGCs) were $86.80\% \pm 2.82\%$, $13.20\% \pm 2.82\%$, $5.60\% \pm 0.25\%$ and $81.19\% \pm 2.57\%$, respectively. From exact counts on serial sections, OGCs, primordial, preantral and antral follicles numerical density were estimated at $(2.11 \pm 0.28) \times 10^6/\text{mm}^3$, $719.57 \pm 18.04/\text{mm}^3$, $71.84 \pm 3.93/\text{mm}^3$ and $17.29 \pm 3.54/\text{mm}^3$, respectively. We estimated that there would be $(2.11 \pm 0.28) \times 10^9$ OGCs, $(719.57 \pm 18.04) \times 10^3$ primordial follicles, $(71.84 \pm 3.93) \times 10^3$ preantral follicles, $(17.29 \pm 3.54) \times 10^3$ antral follicles in one milliliter 3D bioink when 3D encapsulated mice ovarian constructs. The total number of the three stages follicles per ovary were 1791.74 ± 5.77 , 178.88 ± 1.26 , 43.04 ± 1.13 , and the respective total number of OGCs and follicles per ovary were $(5.26 \pm 0.09) \times 10^6$, 2013.66 ± 8.16 .

Conclusions OGCs and follicles can be accurately measured using either the optical or physical disector. The application of these approaches for the study of 3D bioengineered ovary may contribute to a deeper understanding of the artificial ovary.

Background

With the development of biomedical technology, the traditional medicine has changed to regenerative medicine. And tissue engineering is a typical representative of regenerative medicine. Three-dimensional (3D) bio-printing has been applied to tissue engineering and has achieved important milestones^[1-3]. However, 3D bio-printing is by no means a simple stack of cells and bioink, it also requires the construction of printing platform and the design of printing scheme. Therefore, fully understand the structure of the tissue, the distribution of the main cells and the numerical density of cells are of great significance to the computer 3D reconstruction technology.

At present, 3D bioprinting of natural or synthetic polymers to rebuild a bioengineered ovary has been proved to be a promising technique in preserving fertility^[4-5]. But the artificial ovary should imitate the natural ovary and require appropriate follicles and ovarian cells, which are needed for the artificial ovary to survive and develop. Follicle is an important functional structure of ovary, which is composed of an oocyte and many small follicular cells around it. Ovarian granulosa cells (OGCs) is one of the important follicular cells, who play an estrogen-mediated regulatory role and has a supporting in the development and maturation of follicle, and maintain hormonal balance in the ovarian niche^[6-8]. In addition, abnormal apoptosis of OGC is an important mechanism underlying the premature ovarian insufficiency (POI)^[9]. On

the other hand, the type and number of follicles in a delivery scaffold should be optimised. Grafting preantral follicles has a higher follicular survival and growth rate than grafting primordial follicles^[10]. In order to produce mature oocytes after transplantation, a delivery scaffold must include enough follicles but not too many follicles, which should maintain a small size of the scaffold. A small sized scaffold may be conducive to the prevention of ischemic injury and neovascularisation after transplantation^[11]. In view of this, we conducted quantitative studies on OGCs and follicles.

Although two-dimensional (2D) quantitative data can be obtained by morphometric approaches, the use of design-based stereological techniques is preferable in that stereology is an accurate method to obtain 3D quantitative information of microstructure based on the comprehensive observation of 2D slices^[12]. It is uniform and random sampling in organs, slices, field of vision and spatial direction, rather than randomly selecting samples, each part of the study area has the same probability of being selected. The stereological method of counting the number of particles in 3D space is called disector^[13]. The disector consists of two parallel sections (the reference and the look up). An unbiased counting frame is placed in the reference section, the particles were counted if they appeared in the reference section but not in the look up section. The number of particles measured in the reference space in unit volume of one tissue is the numerical density (Nv). Then particles total number was calculated through multiplying the Nv by the reference space total volume^[14]. The disector can provide essentially unbiased 3D data because it is only related to the existence of particles, but has nothing to do with the size, shape and direction of particles. Nowadays, stereology has found even more extensive application in biology and medicine studies. In future research, we try to apply the stereological method to 3D to reconstruct a bioengineered mouse ovary. The measurement of the volume and volume fraction of ovarian cortex, medulla, follicles and OGCs, the numerical density of OGCs and follicles in the cortex of mouse is expected to provide more accurate information for the computer 3D reconstruction technology before 3D printing.

Results

The volume of ovary and corresponding volume fraction

The volume of ovary in C57BL/6J mice at 10-weeks old was $(2.50 \pm 0.32)\text{mm}^3$. And the volume fraction of cortex, medulla, follicles and OGCs were $86.80\% \pm 2.82\%$, $13.20\% \pm 2.82\%$, $5.60\% \pm 0.25\%$ and $81.19\% \pm 2.57\%$, respectively.

The numerical density of OGCs

The diameters of mouse OGCs were $4.98 \pm 1.69 \mu\text{m}$ (Fig. 1a,b). The Nv of OGCs in C57BL/6J mice at 10-weeks old was $(2.11 \pm 0.28) \times 10^6/\text{mm}^3$. We estimated that there would be $(2.11 \pm 0.28) \times 10^9$ OGCs in one milliliter 3D bioink when 3D encapsulated mice ovarian constructs. The total number of OGCs per ovary was $(5.26 \pm 0.09) \times 10^6$ in the paraffin (Table 1).

Table 1

Statistical table of the number of nuclei. "Q" is the whole number of cells selected in the disector height. "P" denotes the total number of the counted frames in all microscopic fields. The number of particles measured in the reference space in unit volume of ovary is the numerical density (Nv). Then cells total number (N) was calculated through multiplying the Nv by the reference space total volume.

	ovarian granulosa cell	primordial follicle	preantral follicle	antral follicle
Q	5581	87	23	5
P	1451	3780	1145	661
Nv(n/mm ³)	(2.11 ± 0.28) × 10 ⁶	719.57 ± 18.04	71.84 ± 3.93	17.29 ± 3.54
N(n)	(5.26 ± 0.09) × 10 ⁶	1791.74 ± 5.77	178.88 ± 1.26	43.04 ± 1.13

The numerical density of primordial, preantral and antral follicle

As shown in Fig. 1c-g, the mean diameters of follicles of the three stages were $29.70 \pm 12.21 \mu\text{m}$, $52.92 \pm 21.12 \mu\text{m}$ and $56.32 \pm 17.05 \mu\text{m}$ respectively. The Nv of primordial, preantral and antral follicle in C57BL/6J mice at 10-weeks old were $719.57 \pm 18.04 /\text{mm}^3$, $71.84 \pm 3.93/\text{mm}^3$ and $17.29 \pm 3.54/\text{mm}^3$, respectively. There would have $(719.57 \pm 18.04) \times 10^3$ primordial follicles, $(71.84 \pm 3.93) \times 10^3$ preantral follicles and $(17.29 \pm 3.54) \times 10^3$ antral follicles in one milliliter 3D bioink when 3D encapsulated mice ovarian constructs. The respective total number of the three stages follicles per ovary were 1791.74 ± 5.77 , 178.88 ± 1.26 , 43.04 ± 1.13 , and the total number of follicles per ovary was 2013.66 ± 8.16 in the paraffin (Table 1).

Discussion

Stereology is essentially an interdisciplinary branch of science about 3D structures, and it has become an essential tool for various fields who need to obtain quantitative 3D microstructural information. In this study, the volume and corresponding volume fraction of mice ovary had been obtained by using the Cavalieri's principle. Then we described the optical disector and physical disector methods to determine the Nv of OGCs and follicles.

The stereological method of counting the number of particles in 3D space is called disector^[13]. Different focal planes in thick histological section are called optical section, and conventional sections are called physical section. The disector realized by using physical and optical section is therefore called physical and optical disector. Large light microscopic structures (such as glomeruli, islets) and tiny electron microscopic structures (such as mitochondria, synapses) should use the physical disector, which should achieve by serial sections encompassing whole cross-sections of one ovary without specialized stereology equipments; the optical disector is suitable for the counting of small particles, such as cell nuclear (less than twenty microns in diameter)^[15], synaptic granules^[16]. In our study, the minimum

diameter of mouse oocytes was more than 10 μm and therefore using the physical disector. In the same way, OGCs using the optical disector (the maximum diameter was less than 10 μm). The main parameter of stereology we chose is the N_v (the number of particles measured in the reference space per unit volume of ovary) in that we can calculate the amount of cells in one milliliter 3D bioink when 3D encapsulated mice ovarian constructs, no matter what shape the structure is printed. In addition, the volume of any structure, regardless of its shape, can be calculated by the Cavalieri's principle^[17], and the total cell number of tissue can be obtained by multiplying the N_v by the volume of tissue^[14]. Meanwhile, we also estimated the volume fraction of cortex, medulla, follicles and OGCs by dot counting method and the corresponding printed volume can be calculated by multiplying the volume of artificial ovary by the corresponding volume fraction, which is conducive to the design of 3D bioengineered ovary printing scheme.

Many researches in the medical field had shown that stereological study had playing an important role in the study of brain^[18], heart^[19], liver^[20], kidney^[21] and so on. They all thought that, the disector method is the preferred method to estimate the number of cells, especially the optical disector, as it ensures that particle counts is not volume weighted and eliminating the necessity for correction factors. The total number of follicles and OGCs we have obtained were also consisted with the previous high-quality researches^[22-23]. Therefore, these data can provide a basis for quantifying normal mice ovary.

Furthermore, different types of bioink and cells, the construction schemes of 3D bio-printing are different, and the purposes of biological printing are different. By changing the cell planting density, applying different types of cells and hydrogels, designing different cell space locations and other experimental conditions, we can deeply study the communication between cells and the interaction between cells and the external environment. We described the volume and volume fraction, the number and N_v of primordial, preantral, antral follicles and OGCs of mice ovary by stereology, to a certain extent, could meet the needs of creating different 3D bio-printing ovary. The follows are only few examples: 1) Increasing number of women of childbearing age with fatal malignant diseases are surviving and the fertility concerns become paramount. Although ovarian tissue cryopreservation with transplantation is a better technique to safeguard fertility, a bioengineered artificial ovary for further transplantation is more promising, as there is a risk of reimplanting malignant cells together with the frozen-thawed tissue^[24]. The safer approach involves bioink encompass either preantral follicles or other level follicles and the amount of encompassed cells can obtain according to the above N_v . 2) Further insights into the impact of mouse follicle stage on graft outcome in an artificial ovary environment, which require accurate number of different levels follicles to encapsulate. 3) Researchers have found that impaired OGCs function is one of the direct causes of POI^[9]. Clinical pharmacologic hormone replacement therapy (pHRT) is the main method, but the mode of pHRT is controversial. Maybe 3D bioengineered ovarian constructs that recapitulate native OGC–oocyte interactions as an alternative approach, which need the volume fraction and accurate N_v of OGC.

However, there still exist serious problems in the application of stereology although most of the standard stereology measurements of volume, volume fraction, surface area, curvature densities and so on are simple point counting upon correct sampling, no need of any expensive instruments. Stereology involves many steps such as correct experimental design, slicing, sampling and software calculation. The deviation of any step will lead to different results in similar studies. For example, Shojafar et al.^[15] and Noori Hassanvand et al.^[25] both used an optical disector with an unbiased sampling frame to estimate the number of primordial, primary, preantral and antral follicles of autografted mice ovaries. However, the large size differences that exist between primordial and later follicles necessitated the use of different methods to determine their respective numbers, and the accuracy measurement of optical disector would be affected if the diameter of nucleus exceeds the thickness of the section. Thus, it is of great importance to know more about the stereology and make more efficient, inexpensive and easy to be understood methods available, which will promote the scientific results validity and unbiased.

Conclusion

Follicles and OGCs can be accurately measured using the suitable disector methods. The application of these approaches for the study of 3D bioengineered ovary may contribute to a deeper understanding of the artificial ovary that regulate ovarian function in normal and dysfunctional conditions.

Materials And Methods

1.

Animals

Wild-type female C57BL/6J mice, n = 6, (SPF (Beijing) Biotechnology Co., Ltd) at 10-weeks old (22 g) were kept on a 12 h light and 12 h darkness regimen conditions with mouse food and water freely available. All procedures that involved animals were approved by the Local Institutional Animal Ethics Committee.

2.

Tissue collection and processing

Daily vaginal smears were taken to ascertain estrus stage. Mice were anesthetized and all ovaries were collected in dioestrus. Ovaries were fixed in Bouin's fluid and then dehydrated using graded alcohols into paraffin wax. Paraffin-embedded ovaries were serially sectioned at 5 μ m and 15 μ m, then stained using immunohistochemistry (follicle stimulating hormone, FSH, a specific marker of OGC) and hematoxylin and eosin (HE).

3.

Estimation of the volume of ovary and the volume fraction of ovarian cortex, medulla, follicles and OGCs

The volume of ovary was performed by the Cavalieri method (Fig. 2): After staining with HE, every 8th section at 5 μm was chosen from a random start (sampling fraction (f) = 1/8) and 16 sections per ovary were selected and examined using a microscope (BX63; Olympus) with 10 \times magnification. The estimation was obtained by the point counting method as follows:

$$V_{\text{ovary}} = \Sigma P_{\text{total}} \times a(p) \times d \times (1/f)$$

Where “ ΣP_{total} ” is the total number of points superimposed on the sections; “ $a(p)$ ” is the area per point, “ d ” is the distance between the sampled sections, and “ (f) ” is the sampling fraction. The volume fraction of each ovary proportion was estimated as follows:

$$V_{\text{medulla}} = \Sigma P_{\text{medulla}} / \Sigma P_{\text{total}}$$

where “ ΣP_{total} ” is the total number of counted points, “ $\Sigma P_{\text{medulla}}$ ”, “ ΣP_{cortex} ” and “ $\Sigma P_{\text{follicle}}$ ” indicates the total number of points superimposed on the medulla, cortex and follicles. Subtract the result of “ $\Sigma P_{\text{follicle}}$ ” from “ ΣP_{cortex} ” is “ ΣP_{OGC} ”. The volume of the ovarian cortex, medulla, follicles and OGCs were estimated through multiplying the “ V_{ovary} ” by the corresponding volume fraction.

4.

Estimation of the numerical density of OGCs: optical disector

By systematic random manner, 10 sections per ovary were chosen from 15 μm thick sections. OGC counts were made using a $\times 100$ oil immersion objective (NA = 0.5) on an Olympus BX63 microscope and a microscope (DP73; Olympus) joined to a computer. The microscope can measure the movement of the stage in the z-axis. By moving the microscope stage in identical distances, microscopic fields were selected. To avoid surface cutting irregularities that may bias the count, the 3 μm from the top of the sections was used as a guard area, and the next 5 μm of the 15 μm section thickness was optically sectioned. Subsequently, two counting frames (measuring 365.26 μm^2 per frame) were superimposed over the reference section and OGCs were counted if they appeared in the unbiased counting frame applied to the reference section and were not intersected by exclusion lines and did not appear in the look up section (Fig. 3). The N_v of OGC was calculated using the following formulas:

$$N_v = \Sigma Q / \Sigma V(\text{dis}), \Sigma V(\text{dis}) = \Sigma P \times a^2 \times h$$

where “ ΣQ ” is the whole number of GC selected in the disector height, “ $\Sigma V(\text{dis})$ ” is the total volume of the disector, “ ΣP ” denotes the total number of the counted frames in all microscopic fields, “ a^2 ” indicates the area of each frame and “ h ” is the height of the disector.

5.

Estimation of the numerical density of primordial, preantral and antral follicles: physical disector

According to the shape, size, growth rate and histological characteristics of follicles, the growth process can be divided into four stages: primordial follicles, preantral follicles, antral follicles and preovulatory

follicles. According to the demand of 3D printing, we made a quantitative study of the follicles in the first three stages. After staining with HE, every 7th section at 5 μm was chosen from a random start (Fig. 4) and examined using a $\times 40$ oil immersion objective (NA = 0.5) on an Olympus BX63 microscope. Sampling tissue sections were traced to define tissue boundaries and then separate unbiased counting frames (measuring 6400 μm^2 for primordial, 16900 μm^2 for preantral and 22500 μm^2 for antral follicles) superimposed on the reference sections were used to count primordial, preantral and antral follicles. Using the CellSens Dimension software (v1.18; Olympus) match fields between the reference section and the consecutive look up section. Oocyte nuclear was counted as the principle that applied in the granulosa cell. About 100 oocytes per ovary were checked, and the Nv was obtained using the above formulas.

6.

Presentation of data

All data are continuous variables and were presented as mean \pm S.E.M.

List Of Abbreviations

List of abbreviations

three-dimensional (3D)
ovarian granulosa cells (OGCs)
premature ovarian insufficiency (POI)
two-dimensional (2D)
numerical density (Nv)
pharmacologic hormone replacement therapy (pHRT)
follicle stimulating hormone (FSH)
hematoxylin and eosin (HE)

Declarations

Ethics approval and consent to participate

All procedures that involved animals in this study were approved by the Local Institutional Animal Ethics Committee.

Consent for publication

The submission of this manuscript has been approved by all authors.

Availability of data and materials

Not applicable.

Competing interests

The authors declare that they have no competing interests.

Funding

Not applicable.

Authors' contributions

XHH, ZWY and JHZ had designed the research. JHZ drafted the manuscript. JHZ, JKZ, YPT and YBS collected all the data. JHZ, JKZ and YPT analyzed the data and made all the figures in this manuscript. XHH had guided the writing. All authors read and approved the final manuscript.

Acknowledgements

The authors would like to thank Dr. Binglei Wang for contributing to the draft manuscript.

Author information

Jia-Hua Zheng¹, Jing-Kun Zhang¹, Yan-Peng Tian¹, Yan-Biao Song², Zhen-Wei Yang³, Xiang-Hua Huang¹

¹Department of Gynecology, ²Department of Central Laboratory, Second Hospital, Hebei Medical University, Shijiazhuang, Hebei, China. ³Morphometric Research Laboratory, North Sichuan Medical College, Nanchong, Sichuan, China.

Corresponding Author: Xianghua Huang

References

1. Kang HW, Lee SJ, Ko IK, Kengla C, Yoo JJ, Atala A. A 3D bioprinting system to produce human-scale tissue constructs with structural integrity. *Nat Biotechnol.* 2016;34:312-9.
2. Osaki T, Uzel SGM, Kamm RD. Microphysiological 3D model of amyotrophic lateral sclerosis (ALS) from human iPS-derived muscle cells and optogenetic motor neurons. *Sci Adv.* 2018;4:eaat5847.
3. Grigoryan B, Paulsen SJ, Corbett DC, Sazer DW, Fortin CL, Zaita AJ. **et al.** Multivascular networks and functional intravascular topologies within biocompatible hydrogels. *Science.* 2019;364:458 – 64.
4. Salama M, Woodruff TK. From bench to bedside: Current developments and future possibilities of artificial human ovary to restore fertility. *Acta Obstet Gynecol Scand.* 2019;98:659 – 64.
5. Fisch B, Abir R. Female fertility preservation: past, present and future. *Reproduction.* 2018;156:F11–27.

6. Liu T, Qin W, Huang Y, Zhao Y, Wang J. Induction of estrogen-sensitive epithelial cells derived from human-induced pluripotent stem cells to repair ovarian function in a chemotherapy-induced mouse model of premature ovarian failure. *DNA Cell Biol.* 2013;32:685 – 98.
7. Liu T, Huang Y, Zhang J, Qin W, Chi H, Chen J. **et al.** Transplantation of human menstrual blood stem cells to treat premature ovarian failure in mouse model. *Stem Cells Dev.* 2014;23:1548-57.
8. Liu W, Xin Q, Wang X, Wang S, Wang H, Zhang W. **et al.** Estrogen receptors in granulosa cells govern meiotic resumption of pre-ovulatory oocytes in mammals. *Cell Death Dis.* 2017;8:e2662.
9. Codacci-Pisanelli G. **Del Pup L, Del Grande M, Peccatori FA.** Mechanisms of chemotherapy-induced ovarian damage in breast cancer patients. *Crit Rev Oncol Hematol.* 2017;113:90 – 6.
10. Chiti MC, Dolmans MM1, Lucci CM, Paulini F, Donnez J, Amorim CA. Further insights into the impact of mouse follicle stage on graft outcome in an artificial ovary environment. *Mol Hum Reprod.* 2017;23:381 – 92.
11. Revel A, Laufer N, Ben Meir A, Lebovich M, Mitrani E. Micro-organ ovarian transplantation enables pregnancy: a case report. *Hum Reprod.* 2011;26:1097 – 103.
12. Howell K, Hopkins N, Mcloughlin P. Combined confocal microscopy and stereology: a highly efficient and unbiased approach to quantitative structural measurement in tissues. *Exp Physiol.* 2002;87:747 – 56.
13. Sterio DC. The unbiased estimation of number and sizes of arbitrary particles using the disector. *J Microsc.* 1984;134:127 – 36.
14. Shojafar E, Soleimani Mehranjani M, Shariatzadeh SMA. Adipose-derived mesenchymal stromal cell transplantation at the graft site improves the structure and function of autografted mice ovaries: a stereological and biochemical analysis. *Cytotherapy.* 2018;20:1324–36.
15. Yang ZW. *Essential Tools for Morphometric Studies of Biological Tissues: Practical Stereological Methods.* **Beijing:** Cornell University Press; 2012. **p.** 97.
16. Peng B, Lin JY, Shang Y, Yang ZW, Wang YP. Plasticity in the synaptic number associated with neuropathic pain in the rat spinal dorsal horn: A stereological study. *Neurosci Lett.* 2010;486:24 – 8.
17. Gundersen HJ, Bendtsen TF, Korbo L, Marcussen N, Møller A, Nielsen K. **et al.** Some new, simple and efficient stereological methods and their use in pathological research and diagnosis. *APMIS.* 1988;96:379 – 94.
18. Kubíková T, Kochová P, Tomášek P, Witter K, Tonar Z. Numerical and length densities of microvessels in the human brain: Correlation with preferential orientation of microvessels in the cerebral cortex, subcortical grey matter and white matter, pons and cerebellum. *J Chem Neuroanat.* 2018;88:22–32.
19. Jafarinezhad Z, Rafati A, Ketabchi F, Noorafshan A, Karbalay-Doust S. Cardioprotective effects of curcumin and carvacrol in doxorubicin-treated rats: Stereological study. *Food Sci Nutr.* 2019;7:3581-8.
20. Paraš S, Janković O, Trišić D, Čolović B, Mitrović-Ajtić O, Dekić R. **et al.** Influence of nanostructured calcium aluminate and calcium silicate on the liver: histological and unbiased stereological analysis. *Int Endod J.* 2019;52:1162-72.

21. Dakovic Bjelakovic M, Vlajkovic S, Petrovic A, Bjelakovic M, Antic M. Stereological study of developing glomerular forms during human fetal kidney development. *Pediatr Nephrol.* 2018;33:817 – 25.
22. Ataya KM, Valeriote FA, Ramahi-Ataya AJ. Effect of cyclophosphamide on the immature rat ovary. *Cancer Res.* 1989;49:1660-4.
23. Myers M, Britt KL, Wreford NG, Ebling FJ, Kerr JB. Methods for quantifying follicular numbers within the mouse ovary. *Reproduction.* 2004;127:569 – 80.
24. Dolmans MM, Masciangelo R. Risk of transplanting malignant cells in cryopreserved ovarian tissue. *Minerva Ginecol.* 2018;70:436 – 43.
25. Noori Hassanvand M, Soleimani Mehranjani M, Shojafar E. Melatonin improves the structure and function of autografted mice ovaries through reducing inflammation: A stereological and biochemical analysis. *Int Immunopharmacol.* 2019;74:105679.

Figures

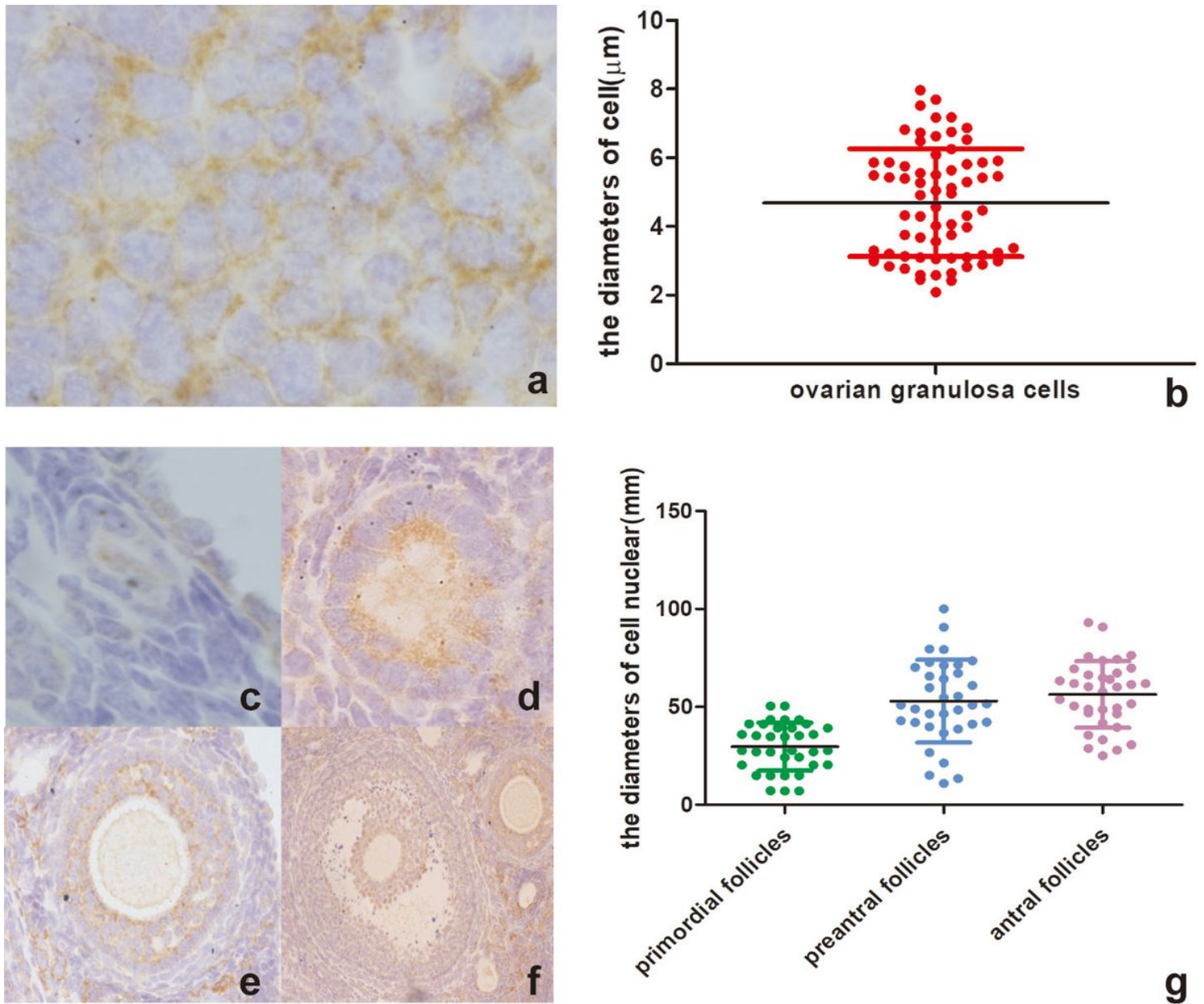


Figure 1

The diameters of ovarian granulosa cells and oocyte nucleus. a. Ovarian granulosa cells. Bar=5µm. The average diameter was $4.98 \pm 1.69 \mu\text{m}$ (b). Primordial follicles were defined as an oocyte surrounded by a layer of squamous granulosa cells (c). Bar=5µm. Preantral follicles include primary follicles and secondary follicles. The former were surrounded by a single layer of cuboidal granulosa cells (d). Bar=5µm. The latter possessed more than one layer of cuboidal granulosa cells and no visible antrum (e). Bar=50µm. Antral follicles possessed a clearly defined antral space (f). Bar=100µm. The mean diameters of follicles of the three stages were $29.70 \pm 12.21 \mu\text{m}$, $52.92 \pm 21.12 \mu\text{m}$ and $56.32 \pm 17.05 \mu\text{m}$ respectively (g).

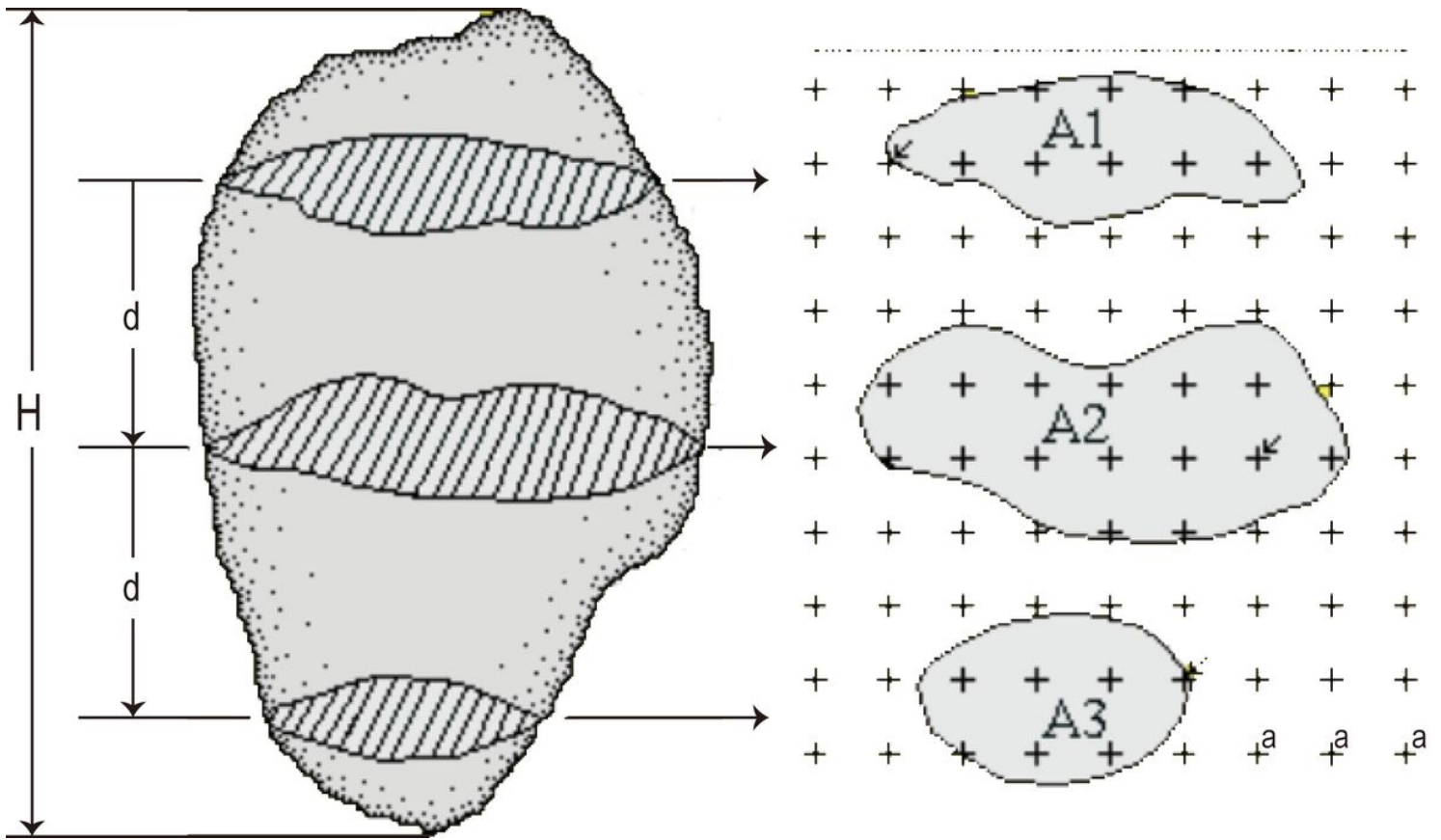
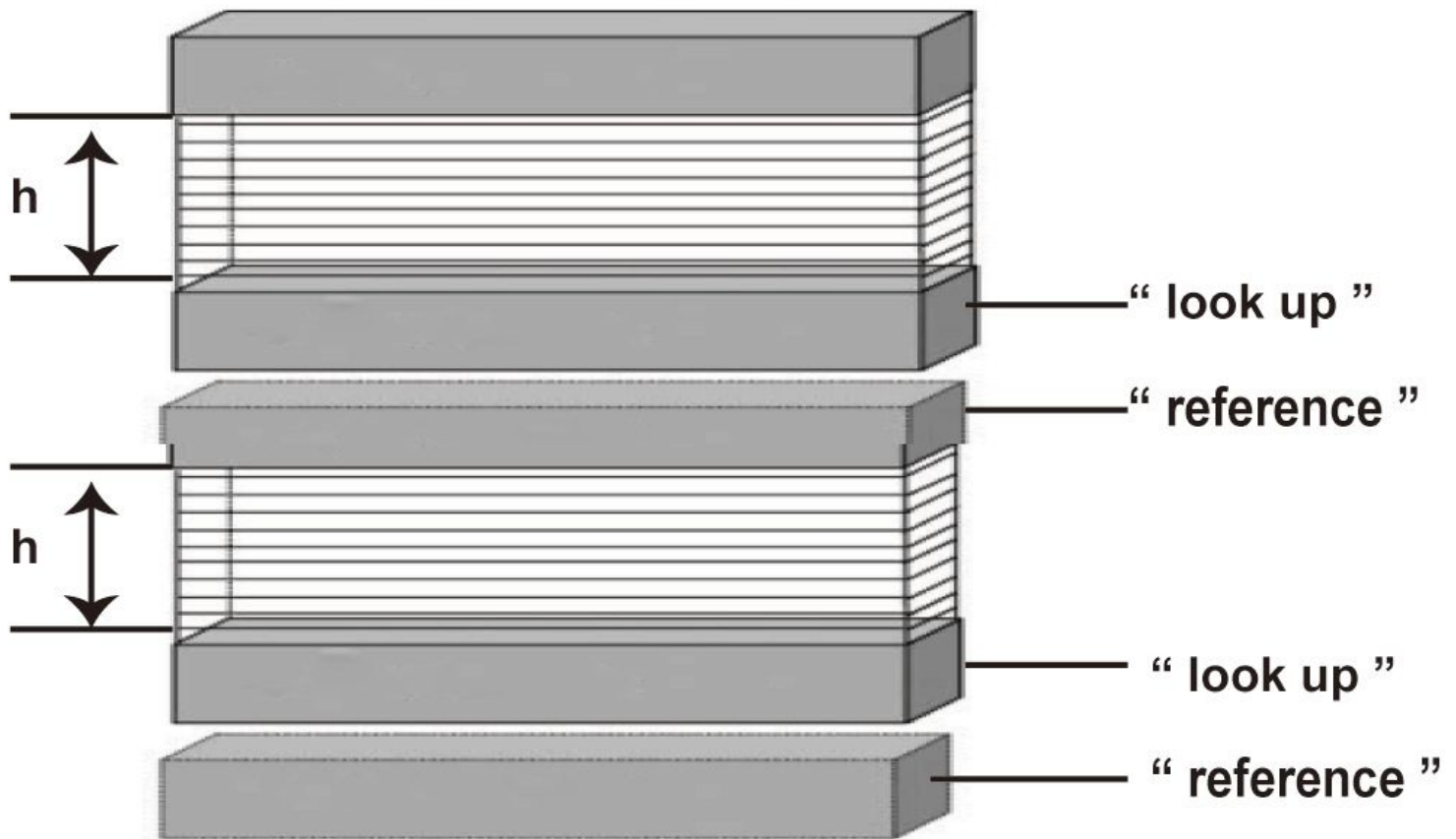


Figure 2

The Cavalieri method used to calculate the volume of the mice ovary, cortex and medulla. 16 sections per ovary from $5\mu\text{m}$ thick sections were randomly selected (sampling fraction (f) = $1/8$) and using point counting method and a microscope with $10\times$ magnification, the number of points superimposed on the images were counted. H is the height of the ovary; d is the distance between the sampled sections; A is the sampled section; a is the side length of point.



the physical disector

Figure 3

Using the optical disector estimate the numerical density of ovarian granulosa cells per ovary. The $3\mu\text{m}$ from the top of the sections was used as a guard area, the next $5\mu\text{m}$ of the $15\mu\text{m}$ section thickness was optically sectioned. The frame itself contains inclusion (green) and exclusion (red) boundaries. Granulosa cells are counted if they appear within the unbiased counting frame and are not intersected by exclusion boundaries and do not appear in the look up section. For example, the particles of No.1-6 in the "reference" can be included as they satisfy the counting criteria and the No.3 touches only the inclusion boundary. The cells of No.7-8 cannot be included as they are touching the exclusion line. Bar= $5\mu\text{m}$.

the optical disector

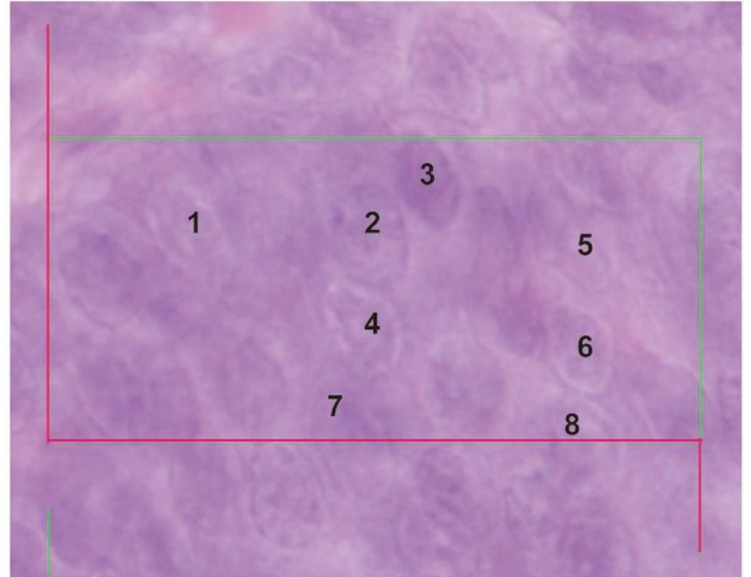
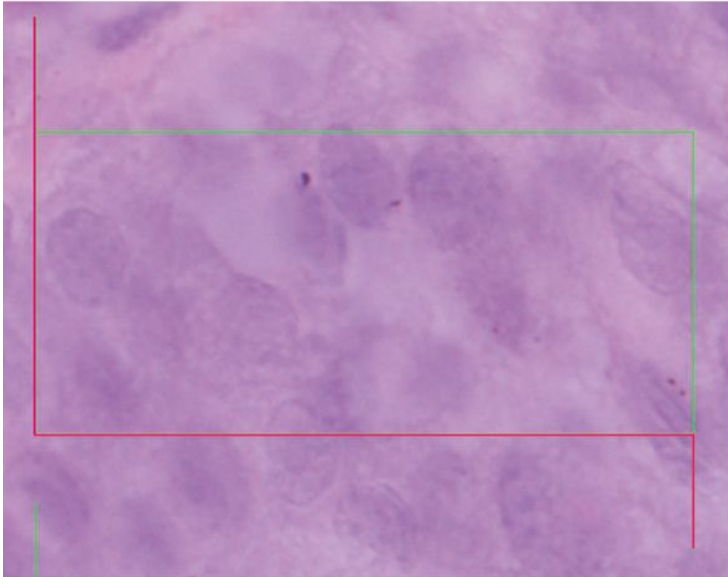
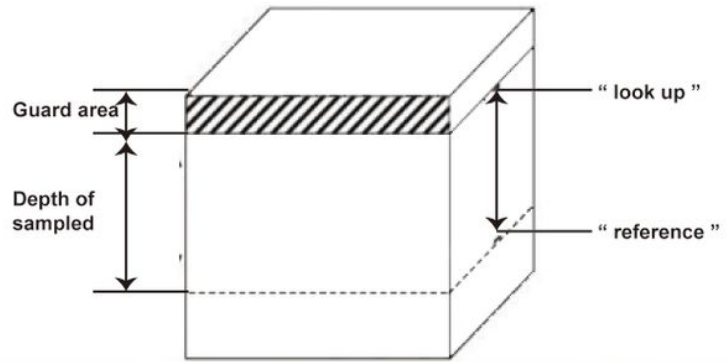


Figure 4

Sampling the ovary to estimate the numerical density of follicles per ovary use the physical disector. The physical disector used a pair of physical sections. Every 8th and 9th section was chose and both sections were aligned a single focal plane. Follicles were counted if they appeared in the reference section but not in the look up section.